FIELDS OF CHARGED PARTICLE BUNCHES IN CHIRAL ISOTROPIC MEDIUM*

S.N. Galyamin[#], A.A. Peshkov and A.V. Tyukhtin[##],
Physical Faculty of St. Petersburg State University, Saint Petersburg, 198504, Russia

Abstract

We study electromagnetic fields produced by charged particle bunches moving in a chiral isotropic medium. Such properties are typical for most of organic matters and some artificial materials (metamaterials). Therefore, this subject is of interest for chemical, biological, and medical applications as well as for study of metamaterials. First, we investigate in detail the field of a point charge. We obtain exact and approximate formulas and develop algorithm for calculation of the point charge field. Further, we use these expressions for calculation of fields produced by finite size bunches. We also present the typical energetic patterns of radiation and spectra of energy losses. Possibilities of using the obtained results for different applications are discussed.

INTRODUCTION

Chirality as an optical phenomenon was known from the late 1811 [1] and was investigated in various aspects during this period. For example, in several late decades, the growth of interest in the electrodynamics of chiral media was connected with possible applications of the artificial chiral structures in the UHF range [2]. Today the prospects of achieving the left-handed properties through the chirality again stimulate the research activity in this area [3]. However, problems with moving charges in chiral media were considered just fragmentary [4,5], with the structure of the total electromagnetic field being practically not analyzed at all. In this paper, we study in detail the electromagnetic field in the situation where the charged particle moves in chiral Condon medium.

ANALYTICAL RESULTS

We use the following symmetrized material relations for the description of chiral medium [2]:

$$\vec{D}_\omega = \varepsilon \vec{E}_\omega - i\kappa \vec{H}_\omega , \quad \vec{B}_\omega = \mu \vec{H}_\omega + i\kappa \vec{E}_\omega , \quad (1)$$

where κ, ε and μ are frequency dependent chiral parameter, dielectric permittivity and magnetic permeability respectively. Introducing vectors $\vec{E}_\omega^+$ and $\vec{E}_\omega^-$ [2,6], so that ($\mathrm{Re}\sqrt{\varepsilon\mu} > 0$)

$$\vec{E}_\omega = \vec{E}_\omega^+ + \vec{E}_\omega^- , \qquad \vec{H}_\omega = \frac{i\sqrt{\varepsilon\mu}}{\mu}\left(\vec{E}_\omega^+ - \vec{E}_\omega^-\right), \quad (2)$$

we obtain the following equations:

$$\Delta\vec{E}_\omega^\pm + \frac{\omega^2 n_\pm^2}{c^2}\vec{E}_\omega^\pm = \frac{2\pi\mu}{\sqrt{\varepsilon\mu}}\left(\frac{-i\omega n_\pm \vec{j}_\omega}{c^2} + \frac{\nabla\rho_\omega^q}{n_\pm} \pm \frac{i\,\mathrm{rot}\,\vec{j}_\omega}{c}\right), \quad (3)$$

where

$$n_\pm = \sqrt{\varepsilon\mu} \pm \kappa , \qquad (4)$$

ρ_ω^q and $\vec{j}_\omega$ are Fourier transforms of charge and current densities. For a point charge moving in accordance with the rule $z = \upsilon t$, we get

$$\rho_\omega^q = \frac{q\delta(x)\delta(y)}{2\pi\upsilon}\exp\left(\frac{i\omega z}{\upsilon}\right), \quad \vec{j}_\omega = \upsilon\rho_\omega^q \vec{e}_z , \qquad (5)$$

$$E_{\omega\rho}^\pm = \frac{iq}{4\upsilon}\frac{\mu}{\sqrt{\varepsilon\mu}}\frac{1}{n_\pm}H_1^{(1)}\left(s_\pm\rho\right)s_\pm\exp\left(i\omega z/\upsilon\right), \qquad (6)$$

$$E_{\omega\varphi}^\pm = \pm\frac{q}{4c}\frac{\mu}{\sqrt{\varepsilon\mu}}H_1^{(1)}\left(s_\pm\rho\right)s_\pm\exp\left(i\omega z/\upsilon\right), \qquad (7)$$

$$E_{\omega z}^\pm = \frac{-q}{4}\frac{\mu}{\sqrt{\varepsilon\mu}}H_0^{(1)}\left(s_\pm\rho\right)\frac{s_\pm^2}{\omega n_\pm}\exp\left(i\omega z/\upsilon\right). \qquad (8)$$

Orthogonal wave vectors $s_\pm$ are determined as follows:

$$s_\pm^2 = \frac{\omega^2}{\upsilon^2}\left(n_\pm^2\beta^2 - 1\right), \quad s_\pm = \sqrt{s_\pm^2}, \quad \mathrm{Im}\,s_\pm > 0 . \qquad (9)$$

Final expressions for the field components can be written in one of the following equivalent forms:

$$E_{\rho,\varphi,z} = 2\,\mathrm{Re}\int_0^{+\infty}d\omega\left(E_{\omega\rho,\varphi,z}^+ + E_{\omega\rho,\varphi,z}^-\right)\exp\left(-i\omega t\right), \quad (10)$$

$$E_{\rho,\varphi,z} = 2\,\mathrm{Re}\int_{-\infty}^{+\infty}d\omega E_{\omega\rho,\varphi,z}^+\exp\left(-i\omega t\right). \qquad (11)$$

The energetic patterns of radiation [7] can be also obtained for the medium under consideration. In the far-field zone, we get ($s_\pm'' = \mathrm{Im}\,s_\pm$):

$$W_{\rho\omega} \approx \frac{q^2}{4\pi\rho}\frac{\mu}{\omega\sqrt{\varepsilon\mu}}\left(\frac{s_+|s_+|}{n_+}\mathrm{F}\left(s_+''\right) + \frac{s_-|s_-|}{n_-}\mathrm{F}\left(s_+''\right)\right), \quad (12)$$

$$W_{z\omega} \approx \frac{q^2}{4\pi^2\upsilon\rho}\frac{\mu}{\sqrt{\varepsilon\mu}}\left(\frac{|s_+|}{n_+}\mathrm{F}\left(s_+''\right) + \frac{|s_-|}{n_-}\mathrm{F}\left(s_+''\right)\right), \quad (13)$$

$W_{\omega\varphi} \approx 0$. Here $\vec{W}$ is the vector of density of total energy, $\vec{W} = \int_{-\infty}^{+\infty}\vec{S}\,dt = \int_0^{+\infty}\vec{W}_\omega\,d\omega$ ($\vec{S}$ is the Poyting vector), $\mathrm{F}(x) = 1$ for $x = 0$ and $\mathrm{F}(x) = 0$ for $x \neq 0$. Energetic patterns are polar plots with $W_\omega = \sqrt{W_{\rho\omega}^2 + W_{z\omega}^2}$ on radial axis and $\theta_W = \mathrm{arctg}\left(W_{\rho\omega}/W_{z\omega}\right)$ on the angular axis.
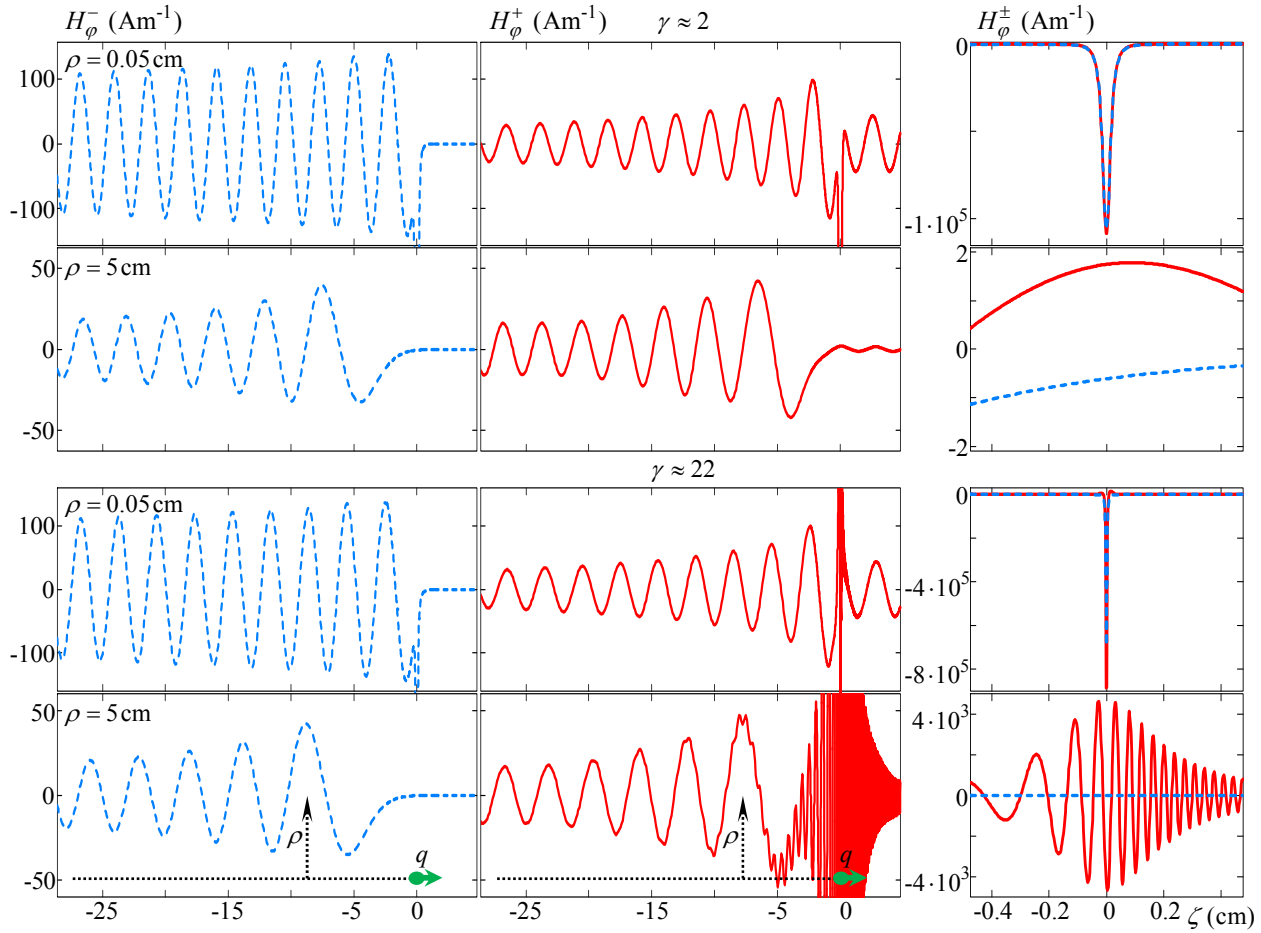
Figure 1: Magnetic field components $H_\varphi^\pm$ of a point charge q versus $\zeta = z - \upsilon t$ for $\gamma < \gamma_c = 10$ (top) and $\gamma > \gamma_c$ (bottom) and different offsets ρ from the charge motion line. Calculation parameters: $q = -1\,\text{nC}$, $\omega_r = \omega_p = 2\pi \cdot 10\,\text{GHz}$, $\omega_0 = 0.1\omega_p$, $\omega_d = 0.001\omega_p$.

The above results are valid for arbitrary frequency dispersion. Below we use the Condon model [2]:

$$\varepsilon(\omega) = 1 + \frac{\omega_p^2}{\omega_r^2 - \omega^2}, \quad \mu = 1, \quad \kappa(\omega) = \frac{\omega\omega_0}{\omega^2 - \omega_r^2}, \quad (14)$$

(ω_p is a "plasma" frequency, ω_r is a resonant frequency and ω_0 is a chiral parameter) which allows calculating both fields and energetic patterns up to the end. We have performed the detailed analysis of properties of integrands in (11) (in the case of weak chirality, $\omega_0 << \omega_r, \omega_p$, and ultrarelativistic motion, $\gamma = 1/\sqrt{1 - \upsilon^2/c^2} >> 1$). The main issue of the performed analysis is that two separated frequency regions of propagating waves exist. The first one exists at arbitrary charge velocity and is located near ω_r while the second one is situated near $\omega_0\gamma^2 >> \omega_r$ and exists for extremely large velocities only,

$$\gamma > \gamma_c, \quad \gamma_c = \omega_p/\omega_0. \quad (15)$$

Moreover, certain parts of these spectral ranges contribute to the field in the domain in front of the charge, resulting in occurrence of the low frequency forerunner and the high frequency forerunner, correspondingly. For numerical calculation, the representation (10) was used. For good performance of the calculating procedure, based on knowledge about integrands' properties we transform the integration path (real axis) in certain way to provide both smooth behavior of integrands and their steepest descent for large values of the integration variable.

NUMERICAL RESULTS

Figure 1 shows typical dependencies of H_φ components (of both the right-hand and left-hand polarizations) on $\zeta = z - \upsilon t$ for different Lorentz factors γ and different offsets ρ from the trajectory. For relatively small charge velocity, $\gamma < \gamma_c$ (Fig. 1, top), the field exhibits oscillating (wave) behavior in the domain behind the charge ($\zeta < 0$) and the strong peak (typical for quasistatic field) near the plane of charge dislocation ($\zeta \approx 0$). For small ρ, the quasistatic components dominates, while for large ρ the wave component practically determines the total field. The aforementioned
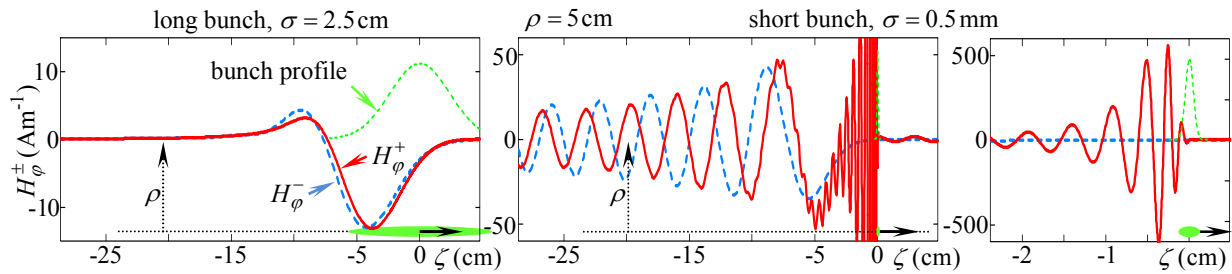
Figure 2: Magnetic fields of one-dimensional longitudinal Gaussian bunches with $\sigma = 2.5\,\text{cm}$ (left) and $\sigma = 0.5\,\text{mm}$ (right) versus $\zeta = z - \upsilon t$. Total bunch charge $q = -1\,\text{nC}$, $\gamma \approx 22$, other parameters coincide with those in Fig. 1.

peculiarities are quite natural for the field of a moving charge in complex media [8]. Important distinction consists in the presence of expressed wave process (forerunner) for the right-hand polarization in front of the charge ($\zeta > 0$). For $\gamma < \gamma_c$ this forerunner oscillates with frequency approaching frequency of the wave field behind the charge, thus we call it the low frequency forerunner. This effect is of most essence for small ρ.

For relatively large velocity, $\gamma > \gamma_c$ (Fig. 1, bottom) and relatively small offset ρ the field behavior practically does not change. Considerable distinctions arise for large offsets ρ where the high frequency spectrum brightly manifest itself in the "$+$" polarization. Now the vicinity of the plane of charge dislocation is decorated with extremely fast oscillations being more frequent for $\zeta > 0$ and less frequent for $\zeta < 0$. The magnitude of the field for $\zeta \approx 0$ becomes around 2-3 orders larger compared with the case $\gamma < \gamma_c$. In the domain in front of the charge ($\zeta > 0$), the high frequency wave process (high-frequency forerunner) dominates the low frequency forerunner for large enough ρ.

Figure 2 shows typical dependencies of the magnetic field components produced by short and long one-dimensional Gaussian bunch with the following charge distribution:

$$\rho^b = \frac{q\delta(x)\delta(y)}{\sqrt{2\pi}\sigma}\exp\left(-\frac{(z-\upsilon t)^2}{2\sigma^2}\right). \tag{16}$$

Plots in Fig. 2 have been calculated though the convolution of the point charge field (10) with (16). The same technique can be utilized for the arbitrary shape bunches as well. As one can see, field of a short bunch practically coincides with the field of point charge for $\zeta < 0$, while for $\zeta > 0$ the field is practically absent. For the long bunch, the wave process reduces practically to one-period oscillation with very low magnitude.

Figure 3 shows typical energy pattern for the field of point charge. The leaf 1 exists at arbitrary γ and its orientation practically does not change with γ. The leaf 2

appears for $\gamma > \gamma_c$ and is oriented closely to the direction of charge motion. The relative role of this leaf increases with further increase in γ.

The described chiral medium can be possibly utilized for particle beam diagnostics via detection of the high-frequency intense radiation produced by the moving particle. If the ultrarelativistic charge flies from considered chiral medium, say, in vacuum through the plane interface, the high frequency radiation will refract at the boundary and penetrate vacuum. Due to the specific direction of this radiation (close to the charge motion direction), almost the whole energy will pass through the interface. This effect can be of interest for particle medicine since the chiral properties are typical for most of biological objects.
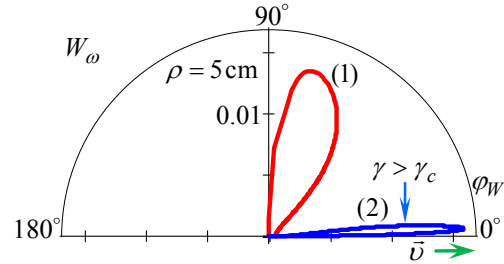

Figure 3: Energetic patterns of the field of the point charge. Calculation parameters are the same as in Fig. 1. W_ω is normalized by multiplier $10^{-13}\,\text{J}\cdot\text{s}\cdot\text{m}^{-2}$.

REFERENCES

[1] B. Kahr, O. Arteaga, ChemPhysChem, 13 (2012) 79.
[2] I.V. Lindell *et al.*, *Electromagnetic Waves in Chiral and Bi-Isotropic Media* (Artech House, 1994).
[3] J.B. Pendry, Science, 306 (2004) 1353.
[4] A.A. Kolomenskii, Zh. Eksp. Teor. Fiz. 24 (1953) 167.
[5] N. Engheta *et al.*, J. Appl. Phys. 68 (1990) 4393.
[6] K.A. Barsukov *et al.*, Tech. Phys. 44 (1999) 328.
[7] J. Lu *et al.*, Opt. Express 11 (2003) 723.
[8] S.N. Galyamin *et al.*, Phys. Rev. E 84 (2011) 056608.